Int. J. Electrochem. Sci., 14 **(2019)** 11237 – 11252, doi: 10.20964/2019.12.35

International Journal of
ELECTROCHEMICAL
SCIENCE
www.electrochemsci.org

Influence of Some Parameters on Membrane-Free Electrodeionization for the Purification of Wastewater Containing Nickel Ions

Xiaolan Shen[1,], Jie Yu[2], Yadong Chen[1], Zhenbo Peng[1], Hao Li[1], Xinmou Kuang[1], Weiqun Yang[1]*

[1] Chemical Engineering Department, Ningbo Polytechnic, Ningbo 315800, China
[2] School of Civil and Environmental Engineering, Ningbo University, Ningbo 315211, China
[*]E-mail: china.xiaolan@163.com

Received: 21 July 2019 / *Accepted:* 20 September 2019 / *Published:* 29 October 2019

Green and efficient treatment of wastewater containing heavy metal is greatly desired. Thus, in this study, membrane-free electrodeionization, which allows the electrical regeneration of the packed resins without the use of membranes and chemicals, was performed for the removal of nickel ions from wastewater. In this MFEDI system, an improved stack configuration was used to prevent nickel hydroxide precipitation and phosphonic acid resin was adopted for adjusting the pH to neutral. The operation parameters (including current density, flow rate during electrical regeneration, and initial nickel concentration) were evaluated in relation to the electrical regeneration of the exhausted resins, the water recovery ratio as well as the energy consumption. The results showed that, the increase of current density and flow rate resulted in better electrical regeneration effect, while the initial nickel concentration had no obvious influence on this process. Their optimal values for energy consumption and water recovery ratio were as follows: current density of 300 A/m^2, flow rate of 10.6 L/h, and initial nickel concentration below 10 mg/L. Under these conditions, the water recovery ratio, energy consumption, pH of the concentrate stream, and conductivity of the dilute stream were, respectively, 87.5%, 4.0 kWh/m^3, 5.9–7.5, and below 0.3 μs/cm.

Keywords: Membrane-free electrodeionization; Electrical regeneration; Precipitation; Nickel containing wastewater; Purification

1. INTRODUCTION

Heavy metals are a major source of pollution, causing global concern. Toxic heavy metals are known to be non-degradable, and can accumulate in living organisms, leading to serious environmental and public health issues [1,2]. Among them, nickel is generally produced in the industrial operations, such as metal electrolysis, electroplating, paper production, mining, and tannery activities [3,4]; excessive ingestion of nickel may cause skin dermatitis, shortness of breath, severe kidney problems and

even skin and lung cancers [5,6]. Besides, since both water and nickel ions are precious, the simultaneous wastewater reuse and nickel recovery are much needed in the industrial field.

Various technologies are currently employed for the nickel removal from wastewater, including chemical precipitation [7,8], adsorption [9-11], ion exchange [12,13], reverse osmosis [14,15], coagulation-flocculation [16,17] and electrodeionization [18-20]. Chemical precipitation is the most widely used process, but its effluent hinders meeting the reuse requirement and the generated sludge induces secondary pollution. Ion exchange is another conventional, high efficiency method. However, the exhausted ion exchange resin should be regenerated with high concentration of alkali and acid. Such a chemical regeneration is laborious, and produces large number of waste water containing acid, alkali and salt ions.

Electrodeionization is a hybrid method: the ion exchange resins are placed in electrodialysis chambers [21-22]. This combination allows the electrochemical regeneration of the ion exchange resins by hydroxide and hydrogen ions, which are formed via electrolysis [23-24]; thus, there is no secondary pollution. Nevertheless, this method presents some drawbacks due to the use of membranes, including membrane fouling, scaling, and high intrinsic costs [25].

Relatively, membrane-free electrodeionization (MFEDI) is an attractive approach for the electrical regeneration of ion exchangers [26–27]. It consists of two steps, alternating with purification and electrical regeneration. During purification, MFEDI is conducted similarly to the conventional ion exchange process and no current is supplied. Through this process, high purity water can be produced. When the resin is exhausted, electricity is supplied, starting the electrical regeneration step; the ion exchange resins are promptly regenerated by hydroxide and hydrogen ions, which come from the water electrolysis and splitting reactions, driven by the electric field. Unlike the simple ion exchange method, no chemicals are needed for the resin regeneration. Compared with conventional electrodeionization, no membranes are required, avoiding their associated limitations. Therefore, MFEDI is more effective than electrodeionization and ion exchange in decreasing both costs and pollution.

However, its stack configuration is not applicable for the treatment of nickel containing wastewater due to the following drawbacks [27]. The reaction between hydroxide ions and nickel ions can lead to nickel hydroxide precipitation; moreover, the concentrate stream may be acidic, which prevents its direct reuse.

In recent studies, nickel hydroxide precipitation has been successfully prevented by improving the MFEDI stack configuration [28] and neutral pH was achieved by introducing a phosphonic acid resin [29]. Nevertheless, the effects of the operation parameters on the ion exchanger regeneration and the MFEDI performance in terms of energy consumption and water recovery ratio are still unknown. Hence, more efforts are required to optimize the results.

The present study investigated the influence of the initial nickel concentration, flow rate during electrical regeneration, and current density on the MFEDI process. In addition, the effectiveness of the stack configuration was further examined. This work differs from a previous study [28] that investigated the feasibility of MFEDI for treatment of nickel containing wastewater for the first time, examined the roles of the resin bed configuration in preventing nickel hydroxide precipitation, and the mechanism of electrical regeneration. In addition, the present study used a layered mixed bed configuration, whose suitability for the nickel containing wastewater treatment has been previously demonstrated [28].

2. EXPERIMENTAL

2.1 Ion Exchangers

Polystyrene-based anion exchanger 550A (strongly basic; Dow, China) and polyacrylic acid-based cation exchanger D113 (weakly acidic; Zhengguang Co., China) were used; the first is a gel type, while the D113 is macroporous. The phosphonic acid resin was synthesized via the Arbuzov reaction [30]; the detailed procedure is described in [26]. Table 1 summarizes the main characteristics of all these ion exchangers. Prior to use, both the phosphonic acid resin and 550A were fully washed with deionized water. D113 was pretreated by soaking in 4% NaOH for 6 h and repeated washing with deionized water, followed by regeneration with 5% HCl to be converted into the hydrogen form and further washing with deionized water.

Table 1. Characteristics of the ion exchangers.

Designation	Type	Matrix	Functional structure	Capacity (eq/L)
550A	strong base	polystyrene	quaternary amine	1.0
D113	weak acid	polyacrylic acid	carboxyl	4.3
650C	strong acid	polystyrene	sulfonyl	2.0
phosphonic acid resin	medium strong acid	polystyrene	phosphonyl	2.9

2.2 Feed Solutions

The experiments were conducted with mixed $NiSO_4/NiCl_2$ solutions. They were prepared with various nickel concentrations (5.0, 10.0, 15.0 and 20.0 mg/L). The $NiCl_2/NiSO_4$ concentration ratio in feed solutions was 2.5, based on the effluent of reverse osmosis (RO) treated nickel electroplating wastewater. All the reagents were of analytical purity.

2.3 Experimental System

The experimental setup described in [28] was adopted. It consisted of a compartment packed with the ion exchange resins and two Pt-coated Ti mesh electrodes (Fig. 1). The compartment and the resin bed were 3 cm in diameter; the electrode gap, corresponding to the resin bed thickness, was 50 cm. Both electrodes had an effective area of 7.1 cm^2. The resin bed was divided into two parts having the same thickness (25 cm); the upper and lower parts were filled with, respectively. the 550A/phosphonic acid resin and the D113/550A mixtures. The volume ratio of the anion exchange resin to the cation exchange resin in the mixtures was 2:1. The ion exchange resins were compressed by a spring. Constant current was provided by a direct current power (Shuanghong Electronics Co., China).

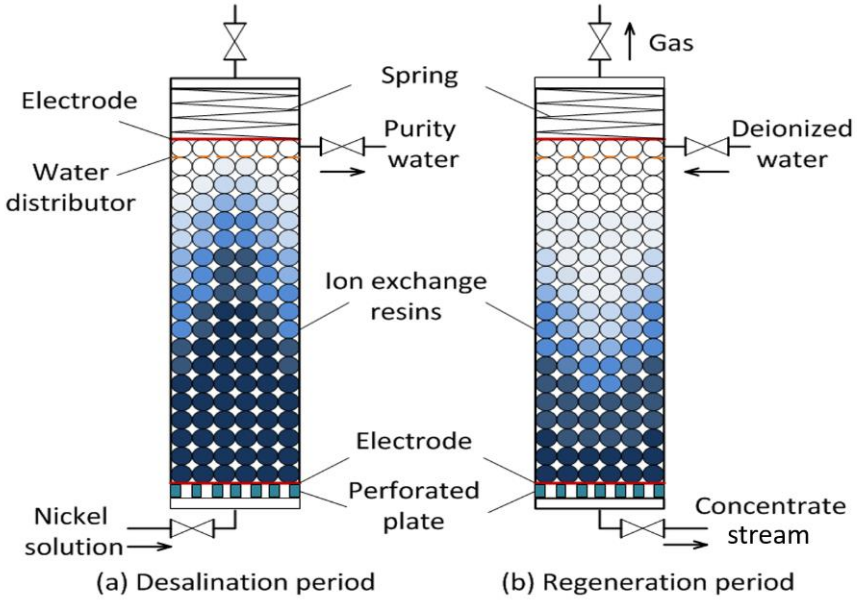

Figure 1. MFEDI setup.

2.4 Wastewater Purification

The two MFEDI processes (purification and electrical regeneration) were operated in batch mode. During purification, the compartment was filled with a pretreated or electrically regenerated ion exchanger, with no electricity. The nickel containing wastewater was continuously treated at an upward flow rate of 7.1 L/h and the dilute stream was obtained at the upper outlet. Salt ions in solution were exchanged with hydrogen or hydroxide ions in the resins, allowing purification of wastewater and production of high purity water (dilute stream). When the conductivity of the dilute stream exceeded 0.3 μs/cm, the electrical regeneration step started.

2.5 Electrical Regeneration of the Resins

During this phase, a constant current density (250, 300 and 350 A/m^2) was supplied and high amounts of hydrogen and hydroxide ions were produced by enhanced water splitting and water electrolysis to be exchanged with the salt ions in the exhausted resins. This condition enabled the electrical regeneration of the ion exchangers, which could be used again for the wastewater purification. A downward flow rate (7.1, 10.6 and 14.2 L/h) was chosen to obtain a concentrate stream with a high nickel concentration for recovery. As shown in Fig. 1(b), deionized water entered the MFEDI system through the upper inlet, and the concentrate stream came out through the lower outlet [31]. Unlike the dilute stream, the concentrate stream was composed of nickel, chloride and sulfate ions, which were released from the resins by electrical regeneration process. The electrical regeneration lasted for 20 min. Thereafter, the purification step started again.

2.6 Analysis

All the experiments were carried out at 298 K. Solutions of both the dilute stream during purification and the concentrate stream during electrical regeneration were collected at predetermined time intervals. The conductivity of the dilute stream, nickel concentration and pH of the concentrate stream, as well as the cell voltage were evaluated: a conductivity meter (Sension 5, Hach, Ameirica) was used to measure the solution conductivity, the nickel concentration was determined using a flame atomic spectrophotometer (AA-6300, Shimadzu, Japan), and the pH was monitored with a pH/ISE meter (Dual Star^{TM}, Orion, Singapore).

3. RESULTS AND DISCUSSION

3.1 Effect of Current Density

Since current density is an important operation parameter, its effect on the MFEDI performance for the electrical regeneration of the resins was investigated; for this purpose, different current densities (0, 250, 300, and 350 A/m^2) were tested. The initial nickel concentration was 10.0 mg/L, the flow rate during electrical regeneration was 7.1 L/h and the purification time for the new resins lasted 83 h. Fig. 2 shows how the nickel concentration in the concentrate stream varied with time without current and after applying a current density of 300 A/m^2.

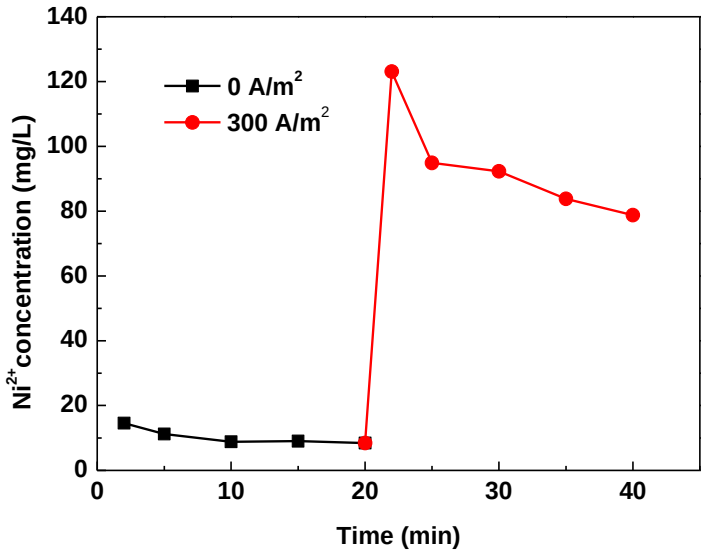

Figure 2. Concentration of the nickel ions in the concentrate stream while using no current and a current density of 300 A/m^2. The flow rate during electrical regeneration and initial nickel concentration were 7.1 L/h and 10.0 mg/L, respectively.

In the first 20 min, no electricity was supplied and the resin was simply regenerated by deionized water in the MFEDI stack. The nickel concentration in the concentrate stream was around 10.0 mg/L, as a consequence of the release of nickel ions from the resin phase to the solution phase; a similar result has been observed by Zhang et al. [20] when performing electrodeionization to purify wastewater

containing Cs^+. After these first 20 min, current was supplied and the nickel concentration promptly increased up to 123.1 mg/L at 22 min, and then, decreased gradually to 78.8 mg/L at 40 min. This indicates that electric current is crucial in the regeneration of exhausted resins. It should be noted that, the concentrate stream has great potential to be reused for industrial activities such as mining and electroplating; thus, our future efforts will be focused on the reuse and recycling of concentrated heavy metal solutions.

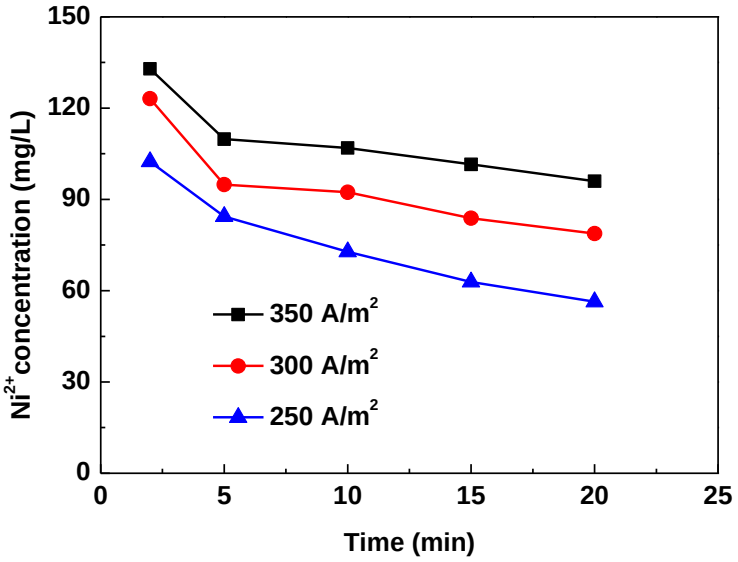

Figure 3. Concentration of the nickel ions in the concentrate stream when applying different current densities. The flow rate during electrical regeneration and initial nickel concentration were 7.1 L/h and 10.0 mg/L, respectively.

Fig. 3 and 4 compare the nickel concentration of the concentrate stream and the voltage, respectively, for the different current densities tested. In all cases using current, the nickel concentration in the concentrate stream decreased during the regeneration process. By mixing all the concentrate stream, the average nickel concentrations observed at 250, 300, and 350 A/m^2 were, respectively, 70.8, 94.7, and 103.2 mg/L; in other words, the higher the current density, the lower the nickel concentration in the concentrate stream. This result can be explained with the following reactions:

$$2H_2O + 2e^- \rightarrow 2OH^- + H_2 \uparrow \quad (1)$$

$$2H_2O - 4e^- \rightarrow 4H^+ + O_2 \uparrow \quad (2)$$

$$H_2O \rightarrow H^+ + OH^- \quad (3)$$

$$R_2\text{–}Ni + 2H^+ \rightarrow 2R\text{–}H + Ni^{2+} \quad (4)$$

$$R\text{–}Cl + OH^- \rightarrow R\text{–}OH + Cl^- \quad (5)$$

$$R_2\text{–}SO_4 + 2OH^- \rightarrow 2R\text{–}OH + SO_4^{2-} \quad (6)$$

where R–H is the cation resin in the hydrogen form, R–OH is the anion resin in the hydroxide form, R_2–Ni is the cation resin in the nickel form, and R–Cl and R_2–SO_4 are the anion resin in, respectively, the chloride and the sulfate form. In the MFEDI stack, when electricity was supplied, reaction (1) might have occurred at the cathode, while reaction (2) could occur at the anode. On the other hand, under a direct electric field, the nickel ions migrated downward (the cathode was on the bottom), while the

chloride and sulfate ions went upward. This resulted in a rapid depletion of ions at the interfaces of the anion and cation exchangers, causing reaction (3) [32]. The hydrogen ions produced by the reactions (2) and (3) could obviously regenerate the cation exchange resin through reaction (4); at the same time, the hydroxide ions produced by the reactions (1) and (3) could regenerate the anion exchanger through the reactions (5) and (6). As the current density increased from 250 to 300 A/m^2, the rates of the reactions (1)-(3) increased and also the nickel concentration did.

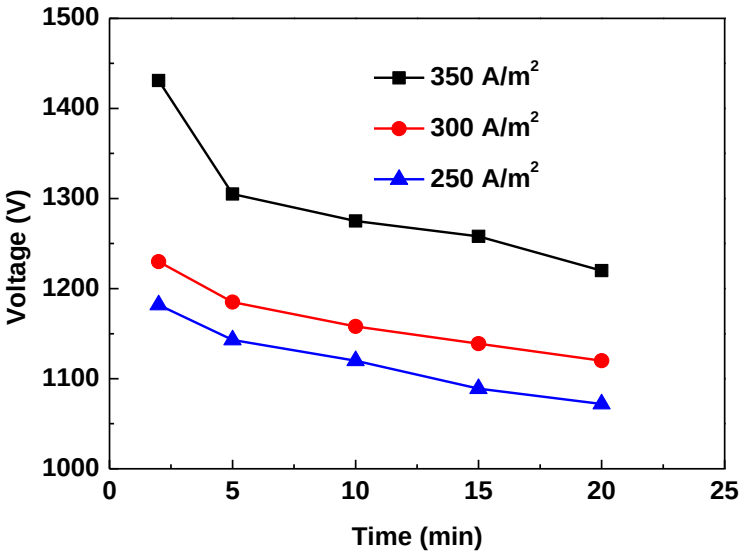

Figure 4. Voltage variations when applying different current densities. The flow rate during electrical regeneration and initial nickel concentration were 7.1 L/h and 10.0 mg/L, respectively.

Fig. 4 shows that the voltage dropped during the regeneration process but increased with the current density supplied; its average values were 1115, 1158, and 1280 V at 250, 300, and 350 A/m^2, respectively. This increase was obviously more significant at higher current densities, which was related to the resin form in the MFEDI system. A previous study [29] has shown that, as the regeneration proceeds, the resins change from the salt form to the hydrogen and hydroxide forms, increasing their conductivity and reducing the voltage of the MFEDI system. Since the salt form of the resins declined more slowly at higher current density, the voltage increased more sharply when the current density raised.

The MFEDI performance was evaluated in terms of water recovery ratio (R, %) and energy consumption (E, kWh/m^3), which were defined as follows:

$$R = \frac{(Q_2 t_2 - Q_1 t_1)}{Q_2 t_2}, \quad (7)$$

where Q_1 is the flow rate during purification (L/h), Q_2 is the flow rate during electrical regeneration (L/h), t_1 is the purification time (h), t_2 is the electrical regeneration time (h);

$$E = \frac{I\overline{U}t_1}{(Q_2 t_2 - Q_1 t_1)}, \quad (8)$$

where I is the electrical current (A) and $\overline{U}$ is the average voltage (V).

Fig. 5 presents the water recovery ratio and energy consumption of the MFEDI system at different current densities. As shown, the water recovery ratio increased gradually with the current density; it was 85.7%, 89.5%, and 90.0% at 250, 300, and 350 A/m^2, respectively. However, the 300 A/m^2 current density led to the lowest energy consumption (4.1 kWh/m^3); while 250 and 350 A/m^2 resulted in energy consumptions of 4.7 and 5.0 kWh/m^3, correspondingly. Therefore, 300 A/m^2 was identified as the appropriate current density for electrical regeneration since it simultaneously provided high water recovery ratio and low energy consumption. Hu et al. [33] and Su et al. [31] reported optimal current densities of 63 and 75 A/m^2, respectively, when using MFEDI for the production of high purity water. The wastewater treated mainly contained monovalent sodium and chloride ions, and the resins absorbed those ions could be easier regenerated. Therefore, the current densities in these studies are much lower.

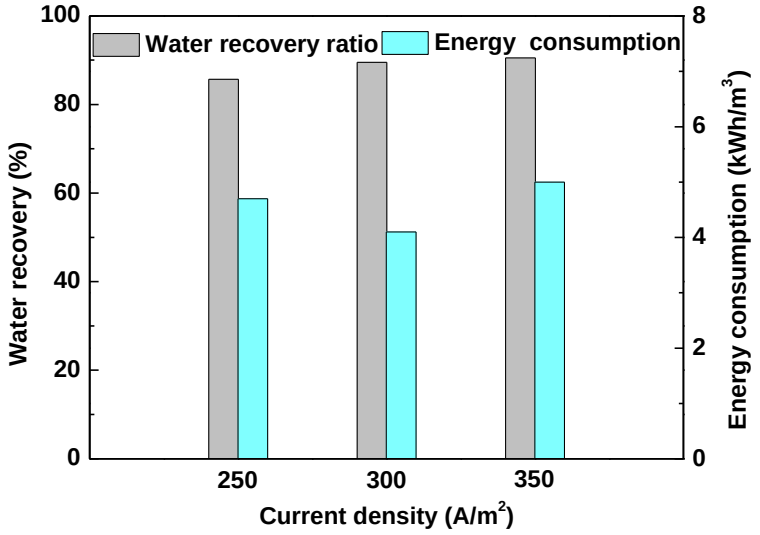

Figure 5. Water recovery ratio and energy consumption of the MFEDI system at different current densities. The flow rate during electrical regeneration and initial nickel concentration were 7.1 L/h and 10.0 mg/L, respectively.

3.2 Effect of Flow Rate during Electrical Regeneration

The flow rate during electrical regeneration is key in the electrical regeneration of ion exchange resins. Thus, three different flow rates (7.1, 10.6, and 14.2 L/h) were used to investigate its effect; the purification time for the new resins lasted 83 h, the initial nickel concentration was 10.0 mg/L and the current density was 300 A/m^2.

Fig. 6 shows the nickel concentration observed in the concentrate stream at the various flow rates. It always dropped during the regeneration process, consistently with that observed in Fig. 3; in addition, it decreased with the flow rate due to the corresponding increased volume of the regeneration solution. The average nickel concentration was 94.7, 80.6, and 60.1 mg/L at flow rates of 7.1, 10.6, and 14.2 L/h, respectively. However, the flow rate of 7.1 L/h resulted in the lowest total amount of regenerated nickel ions (224.1 mg), while the 10.6 and 14.2 L/h flow rates corresponded to values of 264.3 and 284.5 mg. This can be explained as follows. When the flow rate increased, the turbulence in the MFEDI system

increased accordingly, increasing the migration of the ions from the resin to the solution; in addition, this increased flow rate might have decreased the contact time, hindering the adsorption of the nickel ions by the resins [34]. As a result, the total amount of regenerated nickel ions increased.

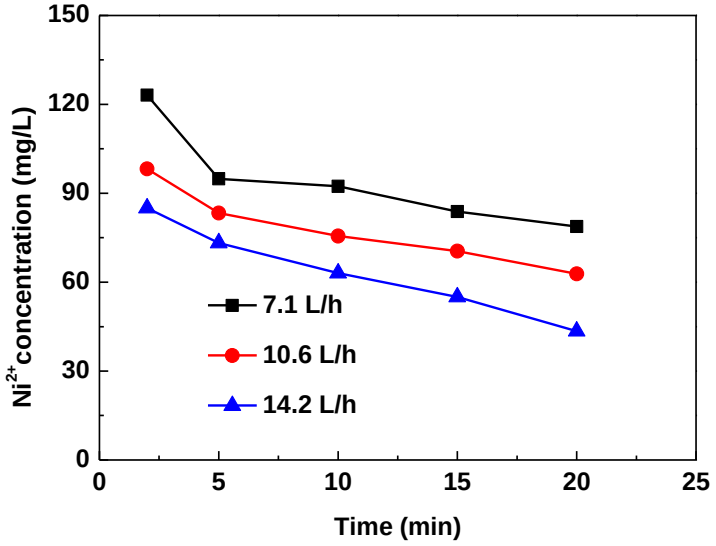

Figure 6. Concentration of the nickel ions in the concentrate stream at different flow rates during electrical regeneration. The current density and initial nickel concentration 300 A/m^2 were 10.0 mg/L, respectively.

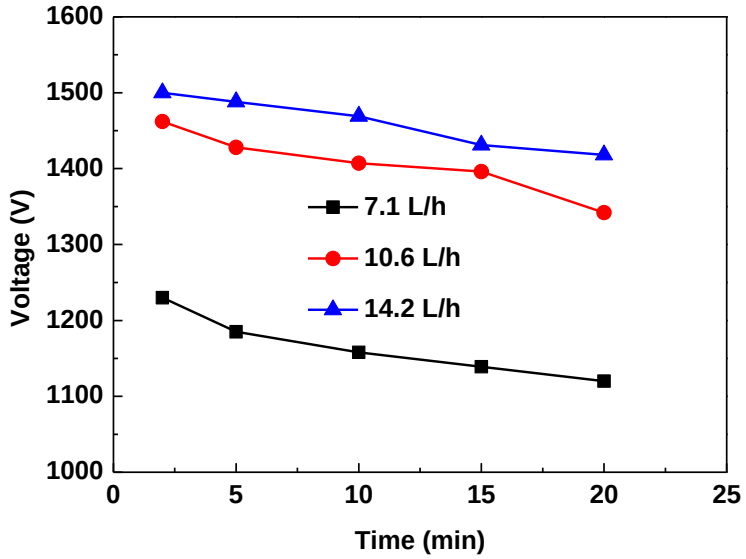

Figure 7. Voltage variations at different flow rates during electrical regeneration. The current density and initial nickel concentration were 300 A/m^2 and 10.0 mg/L, respectively.

Fig. 7 presents the voltage variations at different flow rates during electrical regeneration. The voltage decreased with time but increased with the flow rate; its average values were 1158, 1417, and 1469 V at flow rates of 7.1, 10.6, and 14.2 L/h, respectively. As the nickel concentration in the

concentrate stream decreased with the flow rate, the solution conductivity decreased accordingly. As a result, the voltage increased. This voltage increase with the flow rate was obviously proportional to that of the nickel concentration. When the flow rate increased from 7.1 to 10.6 L/h, the voltage increase was reduced.

The energy consumption and water recovery ratio of the MFEDI system were also evaluated at these flow rates. As shown in Fig. 8, the water recovery ratio decreased with the flow rate; its largest value (89.5%) was obtained at 7.1 L/h, while water recovery ratios of 87.5% and 83.3% were observed at 10.6 and 14.2 L/h, respectively. In addition, the lowest energy consumption (4.0 kWh/m^3) was reached at a flow rate of 10.6 L/h, due to the lower voltage and higher nickel concentration of the concentrate stream, while 4.1 and 4.4 kWh/m^3 values were obtained at 7.1 and 14.2 L/h, respectively. In general, both the water recovery ratio and the energy consumption were very close when the flow rate was 7.1 and 10.6 L/h. Therefore, the appropriate flow rate during electrical regeneration depends on the request; for example, the flow rate suggested for higher water recovery ratios would be 7.1 L/h.

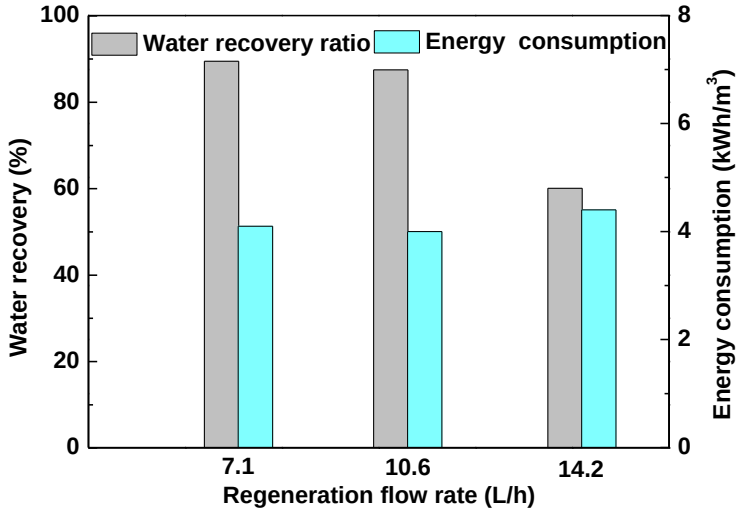

Figure 8. Water recovery ratio and energy consumption of the MFEDI system at different flow rates during electrical regeneration. The current density and initial nickel concentration were 300 A/m^2 and 10.0 mg/L, respectively.

3.3 Effect of Initial Nickel Concentration

To examine the effect of the initial nickel concentration on the electrical regeneration of the resins, this parameter was varied from 5.0 to 20.0 mg/L. Here the flow rate during electrical regeneration was 7.1L/h, the current density was 300 A/m^2. Since the initial nickel concentration was different, the amount of nickel ions absorbed by the resin in the purification step might also vary. It is meaningful to investigate the purification time of the new resin. Thus, the purification time of the MFEDI system with the new resins during purification, and the nickel concentration of the concentrate stream as well as the voltage during regeneration are shown in Fig. 9.

It can be found that, the purification time decreased with the initial nickel concentration (the conductivity of the dilute stream was below 0.3 μS/cm); it was 175, 83, 54, and 39 h for 5.0, 10.0, 15.0, and 20.0 mg/L nickel concentrations, respectively. However, the total amount of nickel ions adsorbed by the resins was barely affected by the initial nickel concentration since its corresponding values were 6.2, 5.9, 5.8, and 5.5 g, according to the flow rate during purification, nickel concentration, and removal time.

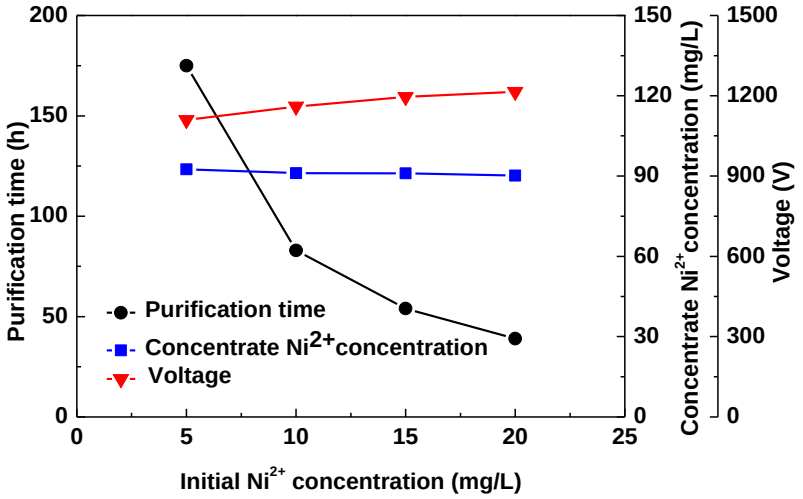

Figure 9. Purification time of the new resins, average nickel concentration in the concentrate stream, and average voltage of the MFEDI system at different initial nickel concentrations. The current density and flow rate during electrical regeneration were 300 A/m^2 and 7.1 L/h, respectively.

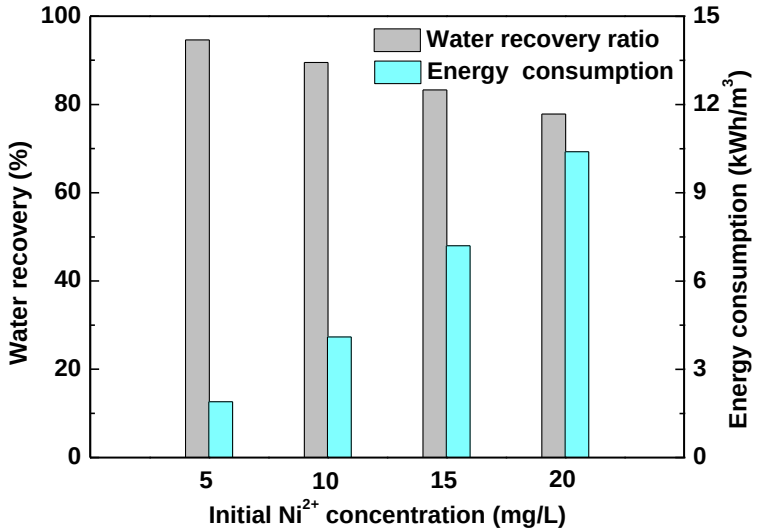

Figure 10. Water recovery ratio and energy consumption of the MFEDI system at different initial nickel concentrations. The current density and flow rate during electrical regeneration were 300 A/m^2 and 7.1 L/h, respectively.

Fig. 9 also reveals that both the nickel concentration in the concentrate stream and the voltage were slightly influenced by the initial nickel concentration; they were around 93.0 mg/L and in the 1110-1215 V range, respectively. The close voltage resulted from the same amount of nickel ions absorbed by the resins.

Fig. 10 illustrates the water recovery ratio and energy consumption of the MFEDI system at the various initial nickel concentrations. Their corresponding values were 94.6%, 89.5%, 83.3%, and 77.8% and 1.9, 4.1, 7.2, and 10.4 kWh/m^3 at 5.0, 10.0, 15.0, and 20.0 mg/L concentrations, respectively. Therefore, to simultaneously decrease the energy consumption and increase the water recovery ratio, the suggested initial nickel concentration should not exceed 10.0 mg/L.

3.4 Nickel Hydroxide Precipitation

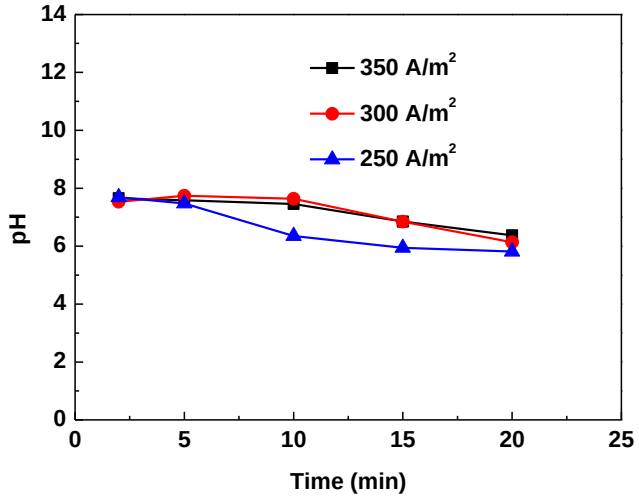

Figure 11. pH of the concentrate stream at different current densities. The flow rate during electrical regeneration and initial nickel concentration were 7.1 L/h and 10.0 mg/L, respectively.

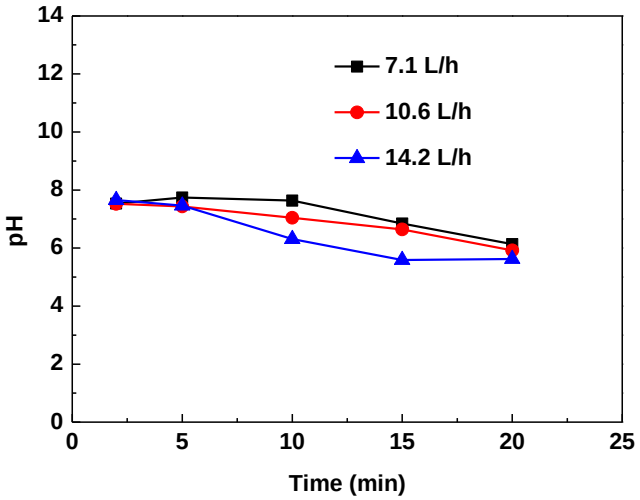

Figure 12. pH of the concentrate stream at different flow rates during electrical regeneration. The current density and initial nickel concentration were 300 A/m^2 and 10.0 mg/L, respectively.

According to the precipitation equilibrium principle, when the ionic product of nickel and hydroxide ($[Ni^{2+}]\cdot[OH^{-}]^2$) exceeds the solubility product of nickel hydroxide (5.50×10^{-16} $(mol/L)^3$ at 298 K [35]), nickel hydroxide precipitation occurs.

Fig. 11-13 show the variation of the pH in the concentrate stream with time for the same experiments represented in Fig. 2, 6, and 9. Steady pH values in the 7.5-7.7 range were initially observed in all the experiments; this was probably due to the high concentration of ions in the anion and cation exchangers, leading to equivalence regeneration of the two types of resins. After about 5 min, the pH gradually decreased down to about 6.1, mainly because of the regeneration difference between the anion and cation exchange resins. The anion exchangers that absorbed monovalent chloride ions were more easily regenerated than the cation ones that absorbed divalent nickel ions; thus, more hydroxide ions were consumed, decreasing the pH of the concentrate stream.

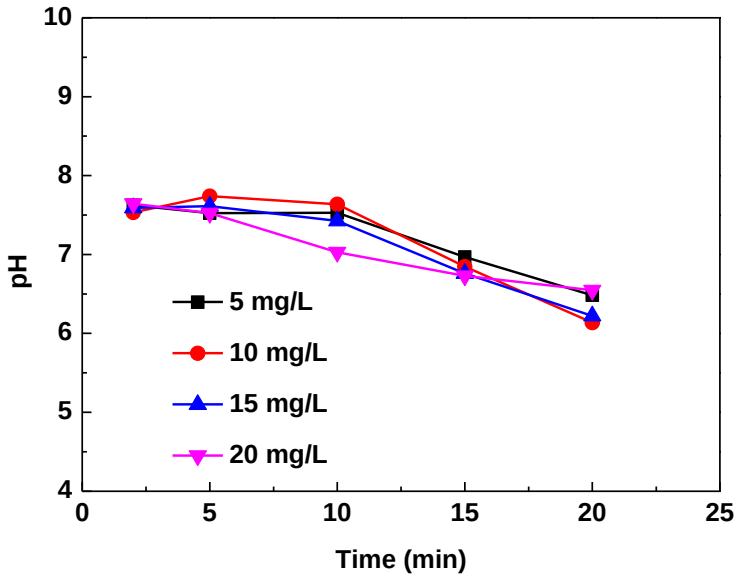

Figure 13. pH of the concentrate stream at different initial nickel concentrations. The current density and flow rate during electrical regeneration were 300 A/m^2 and 7.1 L/h.

Table 2. Ionic product of the nickel and hydroxide ions during electrical regeneration.

t (min)	Varied current density (A/m^2)			Varied flow rate during electrical regeneration (L/h)			Varied initial nickel concentration (mg/L)			
	250	300	350	7.1	10.6	14.2	5	10	15	20
2	4.60×10^{-16}	2.43×10^{-16}	3.76×10^{-16}	2.43×10^{-16}	1.85×10^{-16}	2.65×10^{-16}	3.92×10^{-16}	2.43×10^{-16}	3.25×10^{-16}	3.99×10^{-16}
5	2.78×10^{-16}	4.88×10^{-16}	1.25×10^{-16}	4.88×10^{-16}	1.08×10^{-16}	1.07×10^{-16}	1.91×10^{-16}	4.88×10^{-16}	2.80×10^{-16}	1.81×10^{-16}
10	1.51×10^{-16}	2.93×10^{-16}	6.27×10^{-19}	2.93×10^{-16}	1.72×10^{-17}	4.40×10^{-19}	1.80×10^{-16}	2.93×10^{-16}	1.12×10^{-16}	1.76×10^{-17}
15	8.51×10^{-18}	6.96×10^{-18}	8.27×10^{-20}	6.96×10^{-18}	2.43×10^{-18}	1.40×10^{-20}	1.25×10^{-17}	6.96×10^{-18}	4.72×10^{-18}	4.08×10^{-18}
20	9.11×10^{-19}	2.50×10^{-19}	4.02×10^{-20}	2.50×10^{-19}	7.72×10^{-20}	1.29×10^{-20}	1.21×10^{-18}	2.50×10^{-19}	3.64×10^{-19}	1.69×10^{-18}

Based on the observed pH (Fig. 11-13) and nickel concentration values (Fig. 2, 6 and 9), the ionic product of the nickel and hydroxide ions was calculated; the results are listed in Table 2. The ionic product was consistently lower than the solubility product of nickel hydroxide; in addition, it declined with the regeneration time, which could be attributed to the corresponding decreased nickel concentration and pH in the concentrate stream.

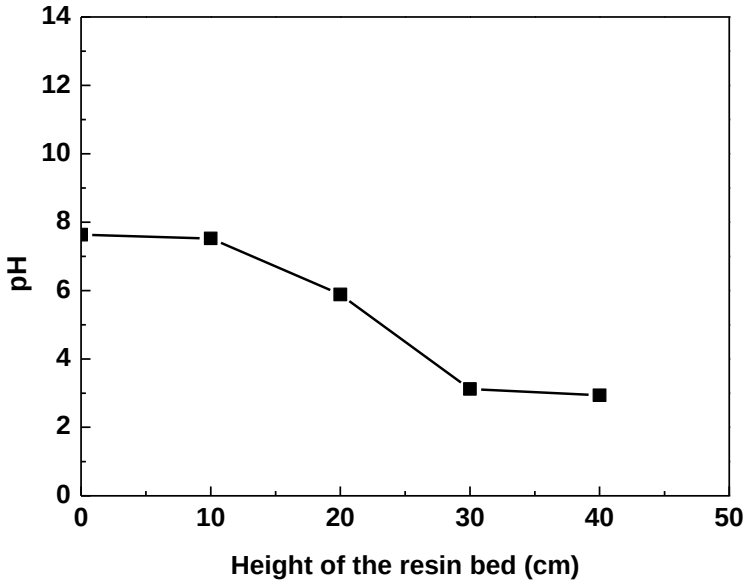

Figure 14. Average pH of the concentrate stream at different height of the resin bed. The current density, flow rate during electrical regeneration, and initial nickel concentration were 300 A/m^2, 7.1 L/h, and 10.0 mg/L, respectively.

On the other hand, since the top electrode was the anode, the hydrogen ions produced by water electrolysis flew downward with the regeneration solution. As a result, the pH of the concentrate stream decreased with the resin bed height, as shown in Fig. 14, where the flow rate during electrical regeneration was 7.1 L/h, the initial nickel concentration was 10.0 mg/L, the current density was 300 A/m^2. Both the highest pH and nickel concentration were obviously obtained in the solution of the cathode, which therefore exhibited the highest ionic product. Thus, there was no nickel hydroxide precipitation during the entire electrical regeneration process.

4. CONCLUSION

Current density, flow rate during electrical regeneration, and initial nickel concentration had different effects on the electrical regeneration of ion exchange resins and, consequently, also on the energy consumption and water recovery ratio. In particular, increasing the current density and flow rate provided better electrical regeneration performance, while the initial nickel concentration had no clear influence on the resin regeneration. The results indicated that the optimal current density to reduce the

energy consumption should be 300 A/m^2, while the suggested flow rate during electrical regeneration to enhance the water recovery ratio would be 10.6 L/h. Besides, decreasing the initial nickel concentration could promote the MFEDI performance and, thus, its value should be lower than 10.0 mg/L.

In the electrical regeneration step, the concentrate stream successfully prevented the nickel hydroxide precipitation, which is the major problem in the practical application of MFEDI for the treatment of heavy metal containing wastewater. Furthermore, under optimal conditions, the concentrate stream was almost neutral and it could be reused directly. Therefore, the results suggested that the improved MFEDI stack configuration could feasibly realize long-term purification of heavy metal containing wastewater.

ACKNOWLEDGEMENT
This work is supported by the General Research Projects of Zhejiang Educational Department (Y201840097), the Ningbo Natural Science Foundation (2018A610280) and the Young Doctoral Innovation Fund of Ningbo Polytechnic (10600300300504).

References

1. O. Rahmanian, M. Dinari and S. Neamati, *Environ. Sci. Pollut. R.*, 25 (2018) 36267.
2. Y. Liu, G.D. Wang, Q. Luo, X.L. Li and Z. Wang, *Mater. Res. Express,* 6 (2019) 025001.
3. S. Gupta and A. Kumar, *Appl. Water Sci.*, 9 (2019) 96.
4. J.M. Yu, J. Zhang, S.Y. Song, H. Liu, Z.Z. Guo and C.L. Zhang, *Colloid Surf., A*, 560 (2019) 84.
5. N. Mokhtari, M. Dinari and O. Rahmanian, *Polym. Int.*, 68 (2019) 1178.
6. D. Jiang, Y.H. Yang, C.T. Huang, M.Y. Huang, J.J. Chen, T.D. Rao and X.Y. Ran, *J. Hazard. Mater.*,373 (2019) 131.
7. Q. Zhang, J. Gao and Y.R. Qiu, *Chem. Eng. Process.*, 135 (2019) 236.
8. H. Hase, T. Nishiuchi, T. Sato, *J. Hazard. Mater.*, 329 (2017) 49.
9. E. Bibaj, K. Lysigaki, J. W. Nolan, M. Seyedsalehi, E. A. Deliyanni, A. C. Mitropoulos and G. Z. Kyzas, *Int. J. Environ. Sci. Te.*, 16 (2019) 667.
10. I. Hachoumi, E. Tatár, V. G. Mihucz, G. Orgován, G. Záray, S.E. Antri and S. Lazar, *Sustain. Chem. Pharm.*, 12 (2019) 100137.
11. P. M. Reddy, C.J. Chang, J.K. Chen, C.F. Huang, C.Y. Chou and M.C. Lee, *React. Funct. Polym.*, 134 (2019) 1.
12. Z.A. Al-Jaser and M.F. Hamoda, *Desalin. Water Treat.*, 157 (2019) 148.
13. A. Ma, A. Abushaikha, S.J. Allen and G. McKay, *Chem. Eng. J.*, 358 (2019) 1.
14. L.A. Richards, B.S. Richards and A.I. Schäfer, *J. Membr. Sci.*, 369 (2011) 188.
15. J.J. Qin, M.N. Wai, M.H. Oo and H. Lee, *Desalination*, 161 (2004) 155.
16. H. Sun, H. Wang, H. Wang and Q. Yan, *Environ. Sci.: Water Res. Technol.*, 4 (2018) 1105.
17. N. Beyazit, *Int. J. Electrochem. Sci.*, 9 (2014) 4315.
18. D. Lee, J.Y. Lee, Y. Kim and S.H. Moon, *Sep. Purif. Technol.*, 179 (2017) 381.
19. H.X. Lu, Y.Z. Wang and J.Y. Wang, *J. Clean. Prod.*, 92 (2015) 257.
20. Y.P. Zhang, L.Wang, S.S. Xuan, X.Y. Lin and X.G. Luo, *Desalination*, 344 (2014) 212.
21. S. Pan, S. Snyder, Y. Lin and P. Chiang, *Environ. Sci-Wat. Res.,* 4 (2018) 613.
22. H.X. Lu, Y.Z. Wang and J.Y. Wang, *J. Clean. Prod.*, 92 (2015) 257.
23. Ö. Arar, Ü. Yüksel, N. Kabay and M. Yüksel, *Desalination,* 342 (2014) 16.
24. P.B. Spoor, L. Koene, W.R. Veen and L.J.J. Janssen, *Chem. Eng. J.*, 85 (2002) 127.
25. K. Dermentzis and K. Ouzounis, *Electrochim. Acta*, 53 (2008) 7123.

26. W.Q. Su, R.Y. Pan, Y. Xiao and X.M. Chen, *Desalination*, 345 (2014) 50.
27. X.L. Shen, T.J. Li, X.P. Jiang and X.M. Chen, *Sep. Purif. Technol.*, 128 (2014) 39.
28. X. L. Shen, Z. Fang, J. Hu and X.M. Chen, *Chem. Eng. J.*, 280 (2015) 711.
29. X.L. Shen and X.M. Chen, *Sep. Purif. Technol.*, 223 (2019) 88.
30. O. Abderrahim, N. Ferrah, M. Didi and D. Villemin, *J. Radioanal. Nucl. Chem.*, 290 (2011) 267.
31. W.Q. Su, R.Y. Pan, Y. Xiao and X.M. Chen, *Desalination*, 329 (2013) 86.
32. J.Y. Hu, Y.J. Chen, L.L. Guo and X.M. Chen, *Desalination*, 365 (2015) 144.
33. J.Y. Hu, Y.J. Chen, L.W. Zhu, Z.H. Qian and X.M. Chen, *Sep. Purif. Technol.*, 164 (2016) 89.
34. S. Bunani, M. Arda and N. Kabay. Desalination, 431 (2018) 100.
35. X. Feng, Z.C. Wu and X.F. Chen, *Sep. Purif. Technol.*, 57 (2007) 257.